Angular dependence of inverse spin–Hall effect induced by spin pumping investigated in a $Ni_{81}Fe_{19}$/Pt thin film

K. Ando* and Y. Kajiwara
Department of Applied Physics and Physico-Informatics, Keio University, Yokohama 223-8522, Japan

S. Takahashi and S. Maekawa
Institute for Materials Research, Tohoku University, Sendai 980-8577, Japan
and CREST, Japan Science and Technology Agency, Kawaguchi, Saitama 332-0012, Japan

K. Takemoto and M. Takatsu
Fujitsu Laboratories Ltd., Morinosato-Wakamiya, Atsugi, Kanagawa, 243-0197, Japan

E. Saitoh
Department of Applied Physics and Physico-Informatics, Keio University, Yokohama 223-8522, Japan
and PRESTO, Japan Science and Technology Agency, Kawaguchi, Saitama 332-0012, Japan
(Received 3 March 2008; published 8 July 2008)

The polar-angular dependence of the magnetization in electromotive force induced by the spin pumping has been investigated for a $Ni_{81}Fe_{19}$/Pt film to examine the model of the inverse spin-Hall effect (ISHE). In the experiment, the magnetization-direction dependence of the electromotive force is estimated directly by the simultaneous measurement of the ferromagnetic resonance field and the electromotive force signal. The experimental results are well reproduced by a calculation based on the Landau-Lifshitz-Gilbert equation combined with the ISHE model.

DOI: 10.1103/PhysRevB.78.014413 PACS number(s): 72.25.Ba, 72.25.Mk, 75.70.Cn, 76.50.+g

I. INTRODUCTION

There has been rapidly growing interest in the field of spintronics, which involves the study of active control and manipulation of the spin degree of freedom in solid-state systems.[1,2] In the research on spintronics, methods for generating and detecting spin currents, a flow of electron spins in a solid are to be established. In this stream, intense theoretical and experimental interests have been focused on the spin-Hall effect (SHE),[3–24] which converts a charge current into a spin current in a solid via the spin-orbit interaction. Theoretically, there are two different models suggested for SHE; one is due to the spin-dependent impurity scattering: the side jump or the skew scattering, which is the extrinsic SHE,[3,4,16,22] and the other is due to the band Berry's phase, which is the intrinsic SHE.[5,6,25] The first observations of SHE are achieved in an *n*-doped bulk semiconductor[11] and in two-dimensional (2D) hole gas.[12]

The inverse process of SHE has the same symmetry as that of the relativistic transformation of the magnetic moment into electric polarization as follows: Consider a magnet with the magnetic moment $\mathbf{M}$ moving at a constant velocity $\mathbf{v}$ with respect to an observer. This motion of the magnet indicates the existence of a "spin current." In the observer's coordinate system, the Lorentz transformation converts a part of this magnetic moment into an electric dipole moment

$$\mathbf{P}' = -\frac{1}{\sqrt{1-(v/c)^2}}(\epsilon_0 \mathbf{v} \times \mathbf{M}), \tag{1}$$

where c and ϵ_0 are the light velocity and the electric constant, respectively. This means that electric polarization perpendicular to the directions of the magnetic moment and the velocity is induced. In this way, electromagnetism and relativity predict that a spin current generates an electric field. According to Eq. (1), however, this electric field is too weak in a vacuum to be detected in reality. In a solid, existence of a pure spin current can be modeled as that two electrons with opposite spins tend to move in opposite directions along the spin-current spatial direction $\mathbf{J}_s$, as shown in Fig. 1. $\boldsymbol{\sigma}$ denotes the spin-current spin polarization. The spin-orbit interaction bends these two electrons in the same direction, and induces a charge current or electromotive force transverse to $\mathbf{J}_s$ and $\boldsymbol{\sigma}$, which is the inverse spin-Hall effect (ISHE). In this effect, $\mathbf{J}_s$, $\mathbf{J}_c$, and $\boldsymbol{\sigma}$ are at right angles to each other (see Fig. 1).

ISHE was recently observed using a spin-pumping method operated by a ferromagnetic resonance (FMR)[14,26] and by a nonlocal method.[13,15,23] ISHE enables the electric detection of spin currents, even in the absence of spin accumulation, and thus plays a crucial role in combining spin-

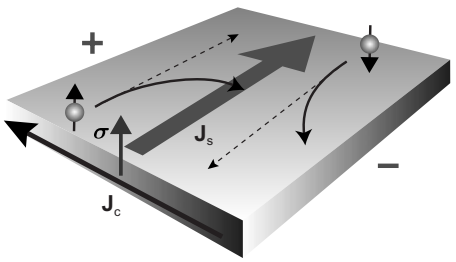

FIG. 1. A schematic illustration of the inverse spin-Hall effect. $\mathbf{J}_c$, $\mathbf{J}_s$, and $\boldsymbol{\sigma}$ denote a charge current, the spatial direction of a spin current, and the spin-polarization vector of a spin current, respectively.

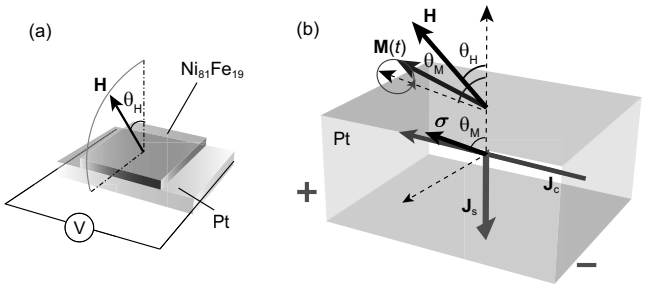

FIG. 2. (a) A schematic illustration of the $Ni_{81}Fe_{19}$/Pt system used in the present study. **H** and θ_H are the external magnetic field vector and the external magnetic field angle to the normal vector of the film plane, respectively. (b) A schematic illustration of the spin pumping and the inverse spin-Hall effect in the present system. **M** is the magnetization in the $Ni_{81}Fe_{19}$ layer. $\mathbf{J}_c$, $\mathbf{J}_s$, and $\boldsymbol{\sigma}$ denote the charge current, the spatial direction of a spin current, and the spin-polarization vector of a spin current, respectively. θ_M is the magnetization angle to the normal vector of the film plane.

tronics with conventional electronics. In particular, the spin-pumping method requires only a simple ferromagnet/paramagnet bilayer film, making it a key technique for generating spin currents in a wide range of sample systems.

The experimental method for detecting ISHE induced by the spin pumping in a ferromagnetic/paramagnetic metal bilayer film is as follows:[14] In the FMR condition, the steady magnetization precession in a ferromagnetic layer is maintained by balancing the absorption of the applied microwave and the dissipation of the spin angular momentum of the magnetization. This dissipation is partly due to the transfer of angular momentum from the local spins to conduction electrons, which polarizes the conduction-electron spins. When a paramagnetic metal is connected to the ferromagnetic metal, this spin polarization propagates into the metal as a spin current, which is the spin pumping operated by FMR.[27–32] The injected spin current in the paramagnetic metal is converted into a charge current by ISHE in the paramagnetic metal. The charge current generated by ISHE causes a charge accumulation at the edges of the paramagnetic-metal layer, or a difference of electric potential between the edges [see Fig. 2(b)]. By measuring the electric potential difference, we can detect ISHE. The direction of the charge current induced by ISHE is expressed in a form (see Fig. 1) as[14]

$$\mathbf{J}_c \parallel (\mathbf{J}_s \times \boldsymbol{\sigma}). \tag{2}$$

To experimentally verify this ISHE model, both the polar-angular and the in-plane angular dependence of the external magnetic field in the ISHE signal should be measured, since $\boldsymbol{\sigma}$ is controllable in terms of the external magnetic field angle. The in-plane field-angle dependence of the ISHE signal has already been reported,[14,33] which is consistent with Eq. (2). However, up to now, the polar-angular dependence has not been measured in the spin-pumping-induced ISHE. In this paper, we report on the polar-angular dependence of magnetization in the spin-pumping-induced ISHE using a $Ni_{81}Fe_{19}$/Pt bilayer film.

II. EXPERIMENTAL PROCEDURE

Figure 2(a) shows a schematic illustration of the sample used in the present study. The sample is a $Ni_{81}Fe_{19}$/Pt bilayer film comprising a 15-nm-thick ferromagnetic $Ni_{81}Fe_{19}$ layer and a 10-nm-thick paramagnetic Pt layer. The Pt layer was fabricated by sputtering on a thermally oxidized Si substrate and then the $Ni_{81}Fe_{19}$ layer was evaporated in a high vacuum. Two electrodes are attached to both ends of the Pt layer.

For the measurement, the sample system is placed near the center of a TE_{011} cavity at which the magnetic-field component of the microwave mode is maximized, while the electric-field component is minimized. During the measurement, a microwave mode with a frequency f=9.441 GHz exists in the cavity, and the external magnetic field **H** is applied at an angle of θ_H to the normal vector of the film plane, as illustrated in Fig. 2(a). When H and f fulfill the FMR condition, a pure spin current with a spin-polarization $\boldsymbol{\sigma}$ parallel to the magnetization in the $Ni_{81}Fe_{19}$ layer is resonantly injected into the Pt layer by the spin pumping[14] [see Fig. 2(b)]. θ_M denotes the angle between the magnetization in the $Ni_{81}Fe_{19}$ layer and the normal vector of the film plane. We measured the FMR signal and the electric-potential difference V between the electrodes attached to the Pt layer with changing θ_H. All the measurements were performed at room temperature. Notable is the fact that in this experimental setup, θ_M is readily estimated at each θ_H value from the values of the FMR fields. Therefore, by simultaneous measurements of the FMR and ISHE signals, the θ_M dependence of the ISHE signal can be investigated.

III. RESULTS AND DISCUSSION

Figures 3(a) and 3(b) show the FMR spectra $dI(H)/dH$, and the dc electromotive force signals V for the $Ni_{81}Fe_{19}$/Pt film under the 200 mW microwave excitation. Here, I denotes the microwave absorption intensity and H_{FMR} is the resonance field [see Fig. 4(a)]. In the V spectra, unconventional signals appear around H_{FMR}. As described in the previous literature, these signals are due mainly to the ISHE induced by the spin pumping.[14,26] This electromotive force signals are well reproduced using Lorentz functions; an example of the fitting result for the electromotive force data observed at θ_H=−90° is shown in Fig. 3(c). This Lorentzian resonance shape indicates that the electromotive force is dominated by ISHE, not by the galvanomagnetic effects.[14,26] The magnitude of the observed electromotive force is found to be proportional to the microwave power, demonstrating that the heating effect due to the microwave application is negligible in the present system.

With changing θ_H, the ISHE signal V changes its sign across θ_H=0 as shown in Fig. 3(b). This is consistent with the prediction of ISHE and the spin pumping; the spin pumping generates a spin current with the spin-polarization-vector $\boldsymbol{\sigma}$ along the magnetization direction. When the magnetic field direction is reversed, Eq. (2) predicts that the $\mathbf{J}_c$ or the electromotive force changes its sign.

The relation between V and θ_M can be discussed by monitoring the θ_H dependence of V and the FMR field H_{FMR} [see

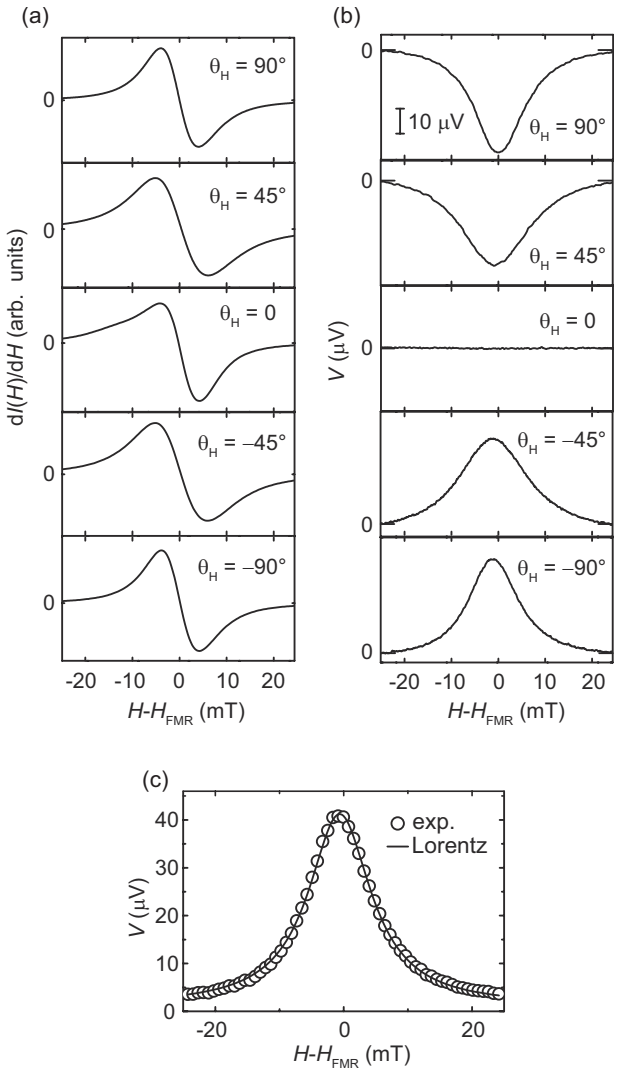

FIG. 3. (a) Field (H) dependence of the FMR signal dI/dH for a $Ni_{81}Fe_{19}$/Pt film. Here, I denotes the microwave absorption intensity. H_{FMR} is the resonance field. From the FMR spectral width at θ_H=90°, the Gilbert damping constant α is estimated to be 0.017. (b) Field dependence of the electric-potential difference V between the electrodes on the Pt layer. (c) A fitting result using a Lorentz function for the V data measured when θ_H=–90°.

Fig. 4(a)]. The θ_M value is calculated from the H_{FMR} data and the saturation magnetization M_s of the $Ni_{81}Fe_{19}$ layer, using the Landau-Lifshitz-Gilbert (LLG) equation.

The dynamics of the magnetization $\mathbf{M}(t)$ in the $Ni_{81}Fe_{19}$ layer under an effective magnetic field $\mathbf{H}_{eff}$ is described by the LLG equation,

$$\frac{d\mathbf{M}(t)}{dt} = -\gamma \mathbf{M}(t) \times \mathbf{H}_{eff} + \alpha \hat{\mathbf{M}}(t) \times \frac{d\mathbf{M}(t)}{dt}. \quad (3)$$

Here, γ, α, and $\hat{\mathbf{M}}$ are the gyromagnetic ratio, the Gilbert damping constant, and the unit vector parallel to the magnetization direction, respectively. First, we consider Eq. (3) in an equilibrium condition, where the equilibrium magnetization direction $\mathbf{M}$ is directed to the z axis [see Fig. 4(b)]. The external magnetic field $\mathbf{H}$ and the static demagnetizing field $\mathbf{H_M}$ induced by $\mathbf{M}$ are taken into account as the effective magnetic field $\mathbf{H}_{eff}$,

$$\mathbf{H}_{eff} = \mathbf{H} + \mathbf{H_M}, \quad (4)$$

where

$$\mathbf{H} = H \begin{pmatrix} 0 \\ \sin(\theta_M - \theta_H) \\ \cos(\theta_M - \theta_H) \end{pmatrix},$$

$$\mathbf{H_M} = -4\pi M_s \begin{pmatrix} 0 \\ \sin\ \theta_M \cos\ \theta_M \\ \cos^2\ \theta_M \end{pmatrix}. \quad (5)$$

The static equilibrium condition, namely $\mathbf{M} \times \mathbf{H}_{eff}$=0 yields an expression, which relates θ_H and θ_M, as

$$\left(\frac{H}{4\pi M_s}\right) \sin(\theta_M - \theta_H) = \sin\ \theta_M \cos\ \theta_M, \quad (6)$$

where H is the strength of the external magnetic field.

We then consider the magnetization $\mathbf{M}(t)$ precession around the z axis, where $\mathbf{M}(t)$=$\mathbf{M}$+$\mathbf{m}(t)$ as shown in Fig. 4(b). $\mathbf{M}$ and $\mathbf{m}(t)$ are the static and the dynamic components of the magnetization, respectively. We take into account the external magnetic field $\mathbf{H}$, the static demagnetizing field $\mathbf{H_M}$ induced by $\mathbf{M}$, the dynamic demagnetization field $\mathbf{H_m}$ induced by $\mathbf{m}(t)$, and the external ac field $\mathbf{h}(t)$ as the effective magnetic field $\mathbf{H}_{eff}$,

$$\mathbf{H}_{eff} = \mathbf{H} + \mathbf{H_M} + \mathbf{H_m} + \mathbf{h}(t), \quad (7)$$

where

$$\mathbf{H_m} = -4\pi m_y \begin{pmatrix} 0 \\ \sin^2\ \theta_M \\ \sin\ \theta_M \cos\ \theta_M \end{pmatrix},$$

$$\mathbf{h}(t) = \begin{pmatrix} h_{ac} \\ 0 \\ 0 \end{pmatrix}. \quad (8)$$

A small precession of the magnetization $\mathbf{m}(t)$ =$(m_x e^{i\omega t}, m_y e^{i\omega t}, 0)$ around the equilibrium direction $\mathbf{M}$ is assumed as a solution of Eqs. (3) and (7). Here ω=$2\pi f$, where f is the microwave frequency. The resonance condition is readily obtained by neglecting the external ac field and the damping term, and by finding the eigenvalue of ω in Eq. (3). By ignoring the second-order contribution of the precession amplitude, m_x and m_y, we find the resonance condition,

$$\left(\frac{\omega}{\gamma}\right)^2 = [H_{FMR} \cos(\theta_M - \theta_H) - 4\pi M_s \cos 2\theta_M] \times [H_{FMR} \cos(\theta_M - \theta_H) - 4\pi M_s \cos^2\ \theta_M]. \quad (9)$$

Here we used Eq. (6). Using Eq. (9) and the experimental H_{FMR} data at θ_H=0 and 90°, the M_s value was estimated. At θ_H=0 and 90°, the magnetization is aligned along the external magnetic field at H_{FMR}, since at θ_H=0 and 90°, H_{FMR} is greater than the magnetization saturation field[34] H_s (H_s

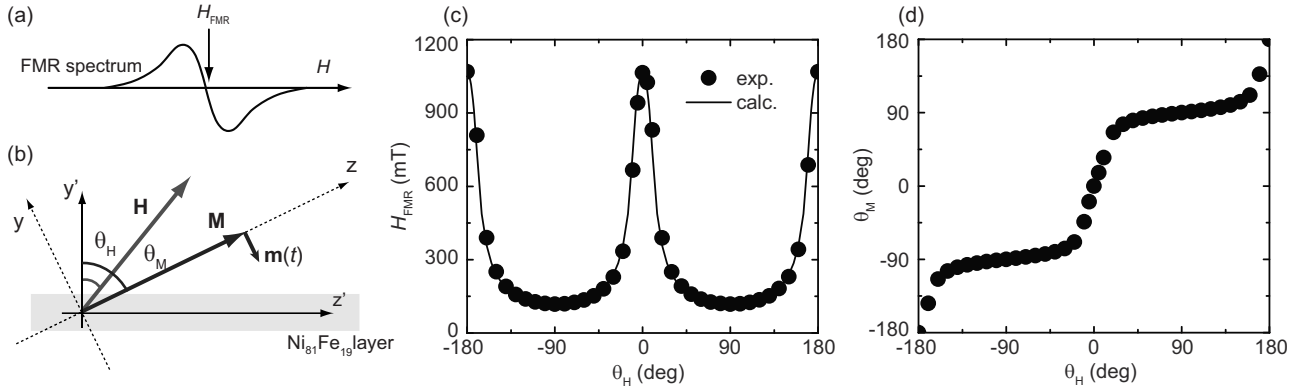

FIG. 4. (a) A schematic illustration of the definition of the resonance field H_{FMR} in the present study. H denotes the external magnetic field. (b) A schematic illustration of the coordinate system used for describing the sample configuration. $\mathbf{M}$ and $\mathbf{m}(t)$ are the static and the dynamic components of the magnetization $\mathbf{M}(t)$. $\mathbf{H}$ is the external magnetic field. θ_H and θ_M are the external-magnetic-field angle and the magnetization angle to the normal vector of the film plane, respectively. (c) The field-angle dependence of H_{FMR}. The filled circles represent the experimental data. The solid line is the numerical solution of Eqs. (6) and (9), using parameters $4\pi M_s$=0.745 T and ω/γ=0.319 T. (d) The field-angle θ_H dependence of the magnetization angle θ_M estimated using Eq. (6).

=745 mT at θ_H=0 and H_s=1.5 mT at θ_H=90°), a situation which is expected for soft-ferromangetic films such as $Ni_{81}Fe_{19}$. Therefore, we obtain the resonance condition

$$\left(\frac{\omega}{\gamma}\right)^2 = (H_{\mathrm{FMR}} - 4\pi M_s)^2, \tag{10}$$

at θ_H=0 and

$$\left(\frac{\omega}{\gamma}\right)^2 = (H_{\mathrm{FMR}} + 4\pi M_s)H_{\mathrm{FMR}}, \tag{11}$$

at θ_H=90°. Substituting the measured H_{FMR} values at θ_H=0 and 90° shown in Fig. 4(c) into these equations, we obtain M_s=59.3 mT and ω/γ=0.319 T. Substituting the measured H_{FMR} values, shown in Fig. 4(c) and M_s into Eq. (6), we finally obtain the θ_H dependence of θ_M, which is shown in Fig. 4(d).

In Fig. 5 we show the field-angle (θ_H) dependence of the ISHE signal V_{ISHE} (filled circles), estimated as the height of the resonance shape in the V spectra (see the inset to Fig. 5). Notable is the drastic change in V_{ISHE} across θ_H=0. This feature is well reproduced by a calculation of V_{ISHE} based on the above model. We assume the isotropic emission of a spin current induced by the spin pumping and the ISHE model, in which spin currents are converted into charge currents whose direction is perpendicular to the spatial direction, and the spin-polarization direction of the spin current, say $\mathbf{J}_c \| (\mathbf{J}_s \times \boldsymbol{\sigma})$. In the phenomenological model of the spin pumping,[28] the spin polarization of the spin current generated by the isotropic-spin pumping is proportional to $\mathbf{m}(t) \times d\mathbf{m}(t)/dt$. In our sample system, therefore, the dc electromotive force V_{ISHE} induced by ISHE and the spin pumping is proportional to the time average of the projection of $\mathbf{m}(t) \times d\mathbf{m}(t)/dt$ to the z' axis [see Fig. 4(b), $\langle \mathbf{m}(t) \times d\mathbf{m}(t)/dt \rangle_{z'}$ because of the relation $\mathbf{J}_c \| (\mathbf{J}_s \times \boldsymbol{\sigma})$]. Making use of $\mathbf{M}(t)$=$\mathbf{M}$+$\mathbf{m}(t)$ in Eq.

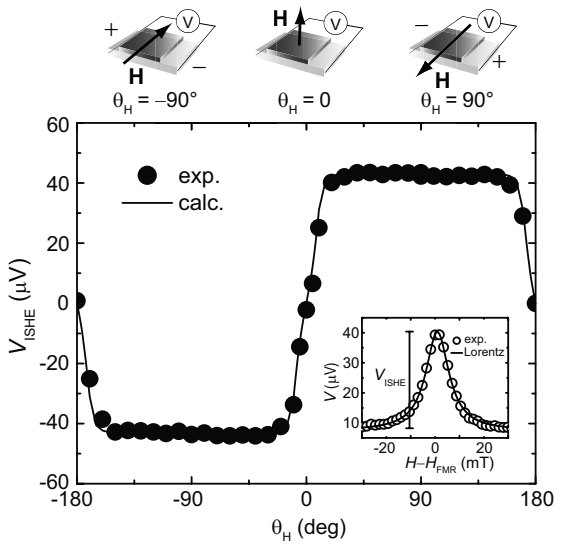

FIG. 5. The field-angle θ_H dependence of the ISHE signal V_{ISHE}. V_{ISHE} is estimated as the height of the resonance shape in V. The filled circles are the experimental data. The solid line is the theoretical curve calculated from Eq. (15).

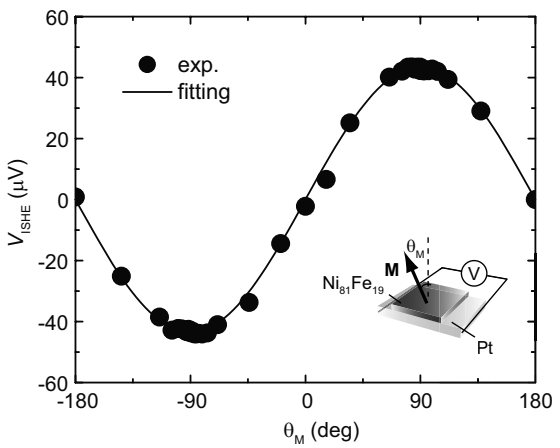

FIG. 6. The θ_M dependence of the ISHE signal V_{ISHE}, where θ_M represents the magnetization angle to the normal vector of the film plane. The solid line shows a fitting result, using a function proportional to sin θ_M.

(3) leads to the equation for the dynamic component $\mathbf{m}(t)$ of the magnetization, in which the external magnetic field, the static demagnetizing field, the dynamic demagnetizing field, and the external ac field are taken into account in $\mathbf{H}_{\text{eff}}$ as described in Eq. (7). Substituting Eq. (7) into the equation for $\mathbf{m}(t)$ and ignoring the second-order contribution of the precession amplitude, we obtain the dynamic component of the magnetization $\mathbf{m}(t)$ as

$$m_x(t) = \frac{h_{ac}(i\tilde{\omega}(\alpha/\gamma) + [\tilde{H}\cos(\theta_M - \theta_H) - \cos 2\theta_M])}{4\pi\cos(\theta_M - \theta_H)[2\tilde{H}\cos(\theta_M - \theta_H) - (\cos 2\theta_M + \cos^2\theta_M)]} \frac{e^{i\omega t}}{(\tilde{H} - \tilde{H}_{\text{FMR}}) + i\dfrac{\alpha\tilde{\omega}}{\cos(\theta_M - \theta_H)}}, \tag{12}$$

$$m_y(t) = \frac{-i\tilde{\omega}h_{ac}}{4\pi\cos(\theta_M - \theta_H)[2\tilde{H}\cos(\theta_M - \theta_H) - (\cos 2\theta_M + \cos^2\theta_M)]} \frac{e^{i\omega t}}{(\tilde{H} - \tilde{H}_{\text{FMR}}) + i\dfrac{\alpha\tilde{\omega}}{\cos(\theta_M - \theta_H)}}, \tag{13}$$

where

$$\tilde{\omega} = \frac{\omega/\gamma}{4\pi M_s} \text{ and } \tilde{H} = \frac{H}{4\pi M_s}. \tag{14}$$

Since $V_{\text{ISHE}} \propto \langle \text{Re}\mathbf{m}(t) \times (\text{d}/\text{d}t)\text{Re}\mathbf{m}(t)\rangle_{z'} = -\omega\,\text{Im}(m_{x'}^* m_{y'}) = -\omega\cos\theta_M\,\text{Im}(m_x^* m_y)$, using Eqs. (12) and (13), a formula for the θ_H dependence of the dc ISHE signal in our setup is obtained as

$$V_{\text{ISHE}} \propto \frac{4\pi M_s \gamma h_{ac}^2}{(4\pi\alpha)^2} \times \frac{\cos\theta_M[\tilde{H}_{\text{FMR}}\cos(\theta_M - \theta_H) - \cos 2\theta_M]}{[2\tilde{H}_{\text{FMR}}\cos(\theta_M - \theta_H) - \cos 2\theta_M - \cos^2\theta_M]^2}. \tag{15}$$

We compared the experimental result with Eq. (15) and found that the experimentally measured field-angle dependence of V_{ISHE} is well reproduced by Eq. (15) as shown in Fig. 5 (solid line). This demonstrates the validity of the ISHE model described in Eq. (2). To show this interpretation explicitly in Fig. 6, V_{ISHE} is replotted as a function of θ_M that is calculated from Eq. (6). Obviously, measured V_{ISHE} is almost proportional to $\sin\theta_M$, demonstrating again that Eq. (2) is relevant to ISHE in the present system.

IV. SUMMARY

In summary, the polar-angular dependence of the magnetization in the inverse spin-Hall effect induced by the spin pumping was investigated. The polar-angular dependence of the magnetization in the electromotive force measured for the $Ni_{81}Fe_{19}$/Pt film is consistent with a calculation based on the model of the inverse spin-Hall effect in which the generated charge current is proportional to $\mathbf{J}_s \times \boldsymbol{\sigma}$, where $\mathbf{J}_s$ and $\boldsymbol{\sigma}$ denote the spatial direction of the spin current and the spin-polarization vector of the spin current, respectively.

ACKNOWLEDGMENTS

The authors thank K. M. Itoh for valuable discussions. This work was supported by a Grant-in-Aid for Scientific Research and Priority Areas Grants from the Ministry of Education, Science, Culture and Sport of Japan, a Strategic Information and Communications R&D Promotion Programme from The Ministry of Internal Affairs and Communications, and NAREGI.

*kazuya_ando@z8.keio.jp

[1] I. Zutic, J. Fabian, and S. D. Sarma, Rev. Mod. Phys. **76**, 323 (2004).
[2] S. A. Wolf, D. D. Awschalom, R. A. Buhrman, J. M. Daughton, S. von Molnar, M. L. Roukes, A. Y. Chtchelkanova, and D. M. Treger, Science **294**, 1488 (2001).
[3] M. I. Dyakonov and V. I. Perel, Phys. Lett. **35A**, 459 (1971).
[4] J. E. Hirsch, Phys. Rev. Lett. **83**, 1834 (1999).
[5] S. Murakami, N. Nagaosa, and S. C. Zhang, Science **301**, 1348 (2003).
[6] J. Sinova, D. Culcer, Q. Niu, N. A. Sinitsyn, T. Jungwirth, and A. H. MacDonald, Phys. Rev. Lett. **92**, 126603 (2004).
[7] E. I. Rashba, Phys. Rev. B **68**, 241315(R) (2003).
[8] J. Schliemann and D. Loss, Phys. Rev. B **69**, 165315 (2004).
[9] E. G. Mishchenko, A. V. Shytov, and B. I. Halperin, Phys. Rev. Lett. **93**, 226602 (2004).
[10] K. Nomura, J. Sinova, T. Jungwirth, Q. Niu, and A. H. MacDonald, Phys. Rev. B **71**, 041304(R) (2005).
[11] Y. K. Kato, R. C. Myers, A. C. Gossard, and D. D. Awschalom, Science **306**, 1910 (2004).
[12] J. Wunderlich, B. Kaestner, J. Sinova, and T. Jungwirth, Phys. Rev. Lett. **94**, 047204 (2005).
[13] T. Kimura, Y. Otani, T. Sato, S. Takahashi, and S. Maekawa, Phys. Rev. Lett. **98**, 156601 (2007).

[14] E. Saitoh, M. Ueda, H. Miyajima, and G. Tatara, Appl. Phys. Lett. **88**, 182509 (2006).
[15] S. O. Valenzuela and M. Tinkham, Nature (London) **442**, 176 (2006).
[16] S. Zhang, Phys. Rev. Lett. **85**, 393 (2000).
[17] V. Sih, W. H. Lau, R. C. Myers, V. R. Horowitz, A. C. Gossard, and D. D. Awschalom, Phys. Rev. Lett. **97**, 096605 (2006).
[18] V. Sih, R. C. Myers, Y. K. Kato, W. H. Lau, A. C. Gossard, and D. D. Awschalom, Nat. Phys. **1**, 31 (2005).
[19] N. P. Stern, S. Ghosh, G. Xiang, M. Zhu, N. Samarth, and D. D. Awschalom, Phys. Rev. Lett. **97**, 126603 (2006).
[20] R. V. Shchelushkin and A. Brataas, Phys. Rev. B **71**, 045123 (2005).
[21] H. Zhao, E. J. Loren, H. M. van Driel, and A. L. Smirl, Phys. Rev. Lett. **96**, 246601 (2006).
[22] J. I. Ohe, A. Takeuchi, and G. Tatara, Phys. Rev. Lett. **99**, 266603 (2007).
[23] T. Seki, Y. Hasegawa, S. Mitani, S. Takahashi, H. Imamura, S. Maekawa, J. Nitta, and K. Takanasni, Nat. Mater. **7**, 125 (2008).
[24] S. Takahashi and S. Maekawa, Phys. Rev. Lett. **88**, 116601 (2002).
[25] H. Kontani and K. Yamada, J. Phys. Soc. Jpn. **63**, 2627 (1994).
[26] H. Y. Inoue, K. Harii, K. Ando, K. Sasage, and E. Saitoh, J. Appl. Phys. **102**, 083915 (2007).
[27] R. H. Silsbee, A. Janossy, and P. Monod, Phys. Rev. B **19**, 4382 (1979).
[28] Y. Tserkovnyak, A. Brataas, and G. E. W. Bauer, Phys. Rev. Lett. **88**, 117601 (2002).
[29] S. Mizukami, Y. Ando, and T. Miyazaki, Phys. Rev. B **66**, 104413 (2002).
[30] Y. Tserkovnyak, A. Brataas, and G. E. W. Bauer, Phys. Rev. B **66**, 224403 (2002).
[31] A. Brataas, Y. Tserkovnyak, G. E. W. Bauer, and B. I. Halperin, Phys. Rev. B **66**, 060404(R) (2002).
[32] M. V. Costache, M. Sladkov, S. M. Watts, C. H. van der Wal, and B. J. van Wees, Phys. Rev. Lett. **97**, 216603 (2006).
[33] K. Harii, K. Ando, H. Y. Inoue, K. Sasage, and E. Saitoh, J. Appl. Phys. **103**, 07F311 (2008).
[34] S. Chikazumi, *Physics of Ferromagnetism*, 2nd ed. (Oxford University, Oxford, 1997).